Hindawi
Mathematical Problems in Engineering
Volume 2022, Article ID 5717924, 16 pages
https://doi.org/10.1155/2022/5717924

Research Article

Application of a Novel Collocation Approach for Simulating a Class of Nonlinear Third-Order Lane–Emden Model

Waleed Adel,[1,2] **Zulqurnain Sabir**,[3] **Hadi Rezazadeh**,[4] **and A. Aldurayhim**[5]

[1]*Department of Mathematics and Engineering Physics, Faculty of Engineering, Mansoura University, Egypt*
[2]*Université Française d'Egypte, Ismailia Desert Road, El Shorouk - Cairo, Egypt*
[3]*Department of Mathematics and Statistics, Hazara University, Mansehra, Pakistan*
[4]*Faculty of Engineering Technology, Amol University of Special Modern Technologies, Amol, Iran*
[5]*Mathematics Department, College of Science and Humanities in Al-Kharj, Prince Sattam Bin Abdulaziz University, Al-Kharj, Saudi Arabia*

Correspondence should be addressed to Waleed Adel; waleedadel85@gmail.com

Received 24 January 2022; Revised 28 April 2022; Accepted 5 May 2022; Published 8 June 2022

Academic Editor: Lei Hou

The present study aims to design a mathematical system based on the Lane–Emden third-order pantograph differential model by using the general forms of the pantograph as well as the Lane–Emden models. The designed model is divided into two types along with the various singularity details at each point. The shape factors and the pantograph points are discussed for each type of the newly designed nonlinear third-order pantograph differential model. The Bernoulli collocation scheme is implemented to find the numerical results of the novel model. To show the reliability of the designed novel nonlinear model, four different variants have been solved. Moreover, the comparison of the obtained results with the exact solutions is presented to check the accuracy of the designed novel model.

1. Introduction

The historical pantograph differential (PD) model is a form of delay differential system that has great importance due to its immense applications in various biological and scientific phenomena. Some examples of these applications are dynamical population models, control problems, communication systems, absorption of light using stellar matter, economical models, engineering, transport, quantum mechanics, electronic systems, infectious diseases, and propagation systems [1–7]. Due to the huge significance of the PD model, many researchers have investigated various efficient techniques to find some accurate solutions to those types of equations. For example, Yuzbas and Karaçayır [8] proposed a generalized form of the multitype pantograph differential equation, which has been solved using a new Galerkin-based approach. In addition, Yuzbas and Karaçayir [9] investigated the application of the same Galerkin-based technique for simulating the results of the pantograph-type Volterra-Fredholm integrodifferential equations with functional upper limit with mixed boundary conditions. Liu and Li in [10] employed a Dirichlet series scheme for finding an analytical solution to the PD model and performing the existence and uniqueness of the suggested algorithm. A Laplace decomposition method has been used in [11] to solve the system of multipantograph differential equations. Yüzbaşi and Ismailov in [12] employed a collocation matrix approach based on the Taylor polynomials for solving the generalized PD equations through the multiple examples that prove the proposed scheme is efficient in acquiring accurate results. Also, the authors of [13] applied a Bessel-based technique for understanding the behavior of the solution of the multipantograph equation systems with mixed conditions. There are other methods for analyzing the PD model such that including the exponential approximation technique [14], shifted Legendre method [15], back-propagated intelligent network technique [16], Gudermannian neural network [17], Hermite polynomial solutions

[18], and Vieta–Lucas series method [19]. These extensive works on the solutions of PD models open the door to exploit the wider applications of similar models of the real-life phenomenon. For more details regarding the applications and techniques for solving the PD models, one may refer to [20–23] and the references therein.

The study of singular differential systems has attracted huge attention from the research community for the last few decades. There are many singular models, out of which Lane–Emden (LE) is one of the historical models that have a singularity at the origin and labels a variety of phenomena in the radiators cooling, gas clouds, cluster galaxies, and polytrophic stars. The LE is such a model that has a variety of applications in dusty fluid systems [24], physical science [25], reactions of catalytic diffusion [26], the density state of a gaseous star [27], isothermal spheres of gas [28], electromagnetic theory [29], catalytic diffusion-based reactions [26], classical mechanics [30], mathematical physics [31], oscillating magnetic fields [32], stellar structure systems [33], and anisotropic continuous media [34]. The wide applications of such models drive the scientists to investigate more into the solutions to these types of equation to understand their behavior which shall reflect more understanding of their applications. For example, Wazwaz [35] adapted a modified version of the Adomian decomposition method to solve the Lane–Emden type equations. Also, a multisingular system of the third-order Emden–Fowler equation has been solved using a neuro-evolution computing algorithm in [36]. In addition, Nisar et al. [37] derived an evolutionary reliable algorithm for solving the second kind of the Lane–Emden problems whereas a similar approach was proposed by Sabir et al. in [38] based on a Morlet wavelet neural network for the same problem. Roul [39] adapted a collocation approach based on the use of B-spline as a basis function to find the solution to a strongly nonlinear singular boundary value problem having possible application in the electro-hydrodynamic flow of fluid. Sabir et al. [40] employed the Gudermannian neural network technique for solving the three-point boundary value problems resulting in some new results for this type of problem. In addition, Roul [41] investigated the solution of a wide class of singular Lane–Emden equations using a novel algorithm based on the combination of the modified Adomian and B-spline collocation approaches through several examples. Several other techniques have been employed for solving different kinds and forms of the singular problem including a stochastic algorithm for solving the nonlinear singular periodic problem [42], the fourth-order B-spline collocation method [43], optimal homotopy technique [44], and other successful methods that found in [45–49]. The mathematical form of the typical singular LE system is presented as [38]

$$\begin{cases} \dfrac{d^2\Psi}{dx^2} + \dfrac{\gamma}{x}\dfrac{d\Psi}{dx} + h(\Psi) = g(x), \\ \Psi(0) = A, \\ \dfrac{d\Psi(0)}{dx} = 0. \end{cases} \tag{1}$$

In the above equation, $\gamma \geq 1$ indicates the shape factor, while $x = 0$ represents the singular point at the origin and A is a constant value. The current work intends to propose an extension to the second-order Lane–Emden pantograph delay differential model presented by Adel and Sabir [50] to the third-order nonlinear pantograph differential Lane–Emden (PD-LE) model.

Over the past few years, Bernoulli collocation (BC) techniques have played an important role to solve different types of application-based problems. Many researchers worked to expand the BC technique to handle those challenges that arise in different areas of science and engineering. For example, Tohidi and Kilicman proposed a BC scheme to solve the generalized form of the PD model [51]. A modified version of the BC method was designed to find an approximate solution to a higher-order complex differential equation in a rectangular domain [52]. The accurate results of the static beam problem have been obtained by using the BC scheme [53]. Toutounian et al. [54] applied the BC scheme for solving the boundary value problems arising in the variation calculus. The study of a few more famous problems is presented by using the BC scheme such those including time-fractional cable equation [55], fourth-order Sturm–Liouville problem [56], stochastic Itô–Volterra integral equations of Abel type [57], and nonlinear two-dimensional Volterra–Fredholm integral equations of Hammerstein type [58].

The main motivation of this paper is to investigate the solution of a general form of the third-order Lane–Emden equation due to its continuous and important application in the real world. In addition, the applications of collocation methods and their ability to provide fast and accurate solutions to different models were one of the main reasons to simulate such an important model to understand more about their dynamics. Also, third-order equations are difficult in finding their solutions, and thus, the addressed method succeeded in achieving highly accurate results. The presented new method based on the Bernoulli collocation approach adheres to several advantages in finding the solution to such models over other existing techniques since it is a fast, straightforward, and simple to apply method. Only a few numbers of bases are considered to achieve high accuracy, and the computational cost for finding these solutions is low. It is worth mentioning that this is the first time that this type of model is examined using this novel technique.

In this work, the numerical investigations of the newly designed hybrid pantograph–LE-based model have been accomplished via the BC approach. Some novel aspects of the designed novel system are described as follows:

(i) A novel design of nonlinear pantograph differential Lane–Emden is proposed using the pantograph differential and standard Emden–Fowler equation

(ii) The designed model is divided into two categories along with the formulation of a differential system

(iii) The values of the shape factors, pantograph terms, and singular points at origin are provided for both categories of the novel-designed model

(iv) Two different numerical nonlinear variants of each category have been discussed using the BC scheme

(v) The comparison of the proposed results from the BC scheme is presented to check the correctness of the novel designed system

The rest of the paper parts are organized as follows: Section 2 designates the construction of the designed model. Section 3 presents the function approximation, fundamental relations, Bernoulli operational matrix, BC scheme, and a few related theorems. Section 4 describes the results and discussions. Conclusions and future research guidance are listed in the last section.

2. Construction of the Third-Order PD-LE Model

This section describes the third-order PD-LE system, which is designed by using the pantograph differential and typical LE models. The novel third-order PD-LE system is divided into two categories, and the detail of each class is presented along with its mathematical procedures. The shape factors, pantographs, and singular points are also discussed based on the novel model. For the derivation of the novel nonlinear third-order PD-LE equation, the mathematical formulation is expressed as

$$\begin{gathered} x^{-k}\frac{d^q}{dx^q}\left(x^k\frac{d^p}{dx^p}\Psi(\alpha x)\right)+\Psi^\nu(x)=g(x),\\ \Psi(0)=A_1,\\ \frac{d\Psi(0)}{dx}=A_2,\\ \frac{d^2\Psi(0)}{dx^2}=A_3, \end{gathered} \tag{2}$$

where k, A_1, A_2, and A_3 are a positive real number. To find the nonlinear PD-LE model, p and q are integer values that must be fixed and written as

$$q+p=3, \quad q,p\geq 1. \tag{3}$$

The following two possibilities that satisfy the above (3) are written as

$$\begin{aligned} q&=2,\\ p&=1, \end{aligned} \tag{4}$$

$$\begin{aligned} q&=1,\\ p&=2. \end{aligned} \tag{5}$$

Using (3) and (4), the mathematical form of the model (2) is categorized as

Category 1: Using (2) in (4), the updated form of the model becomes as

$$x^{-k}\frac{d^2}{dx^2}\left(x^k\frac{d}{dx}\Psi(\alpha x)\right)+\Psi^\nu(x)=g(x), \tag{6}$$

and then, by calculating the derivative, the obtained form is given as

$$\begin{aligned} \frac{d^2}{dx^2}\left(x^k\frac{d}{dx}\Psi(\alpha x)\right)&=\alpha^3x^k\frac{d^3}{dx^3}\Psi(\alpha x)\\ &\quad+2\alpha^2kx^{k-1}\frac{d^2}{dx^2}\Psi(\alpha x)\\ &\quad+\alpha k(k-1)x^{k-2}\frac{d}{dx}\Psi(\alpha x). \end{aligned} \tag{7}$$

Substituting the expression (7) into the equation (2) gives the third-order nonlinear PD-LE; that is,

$$\begin{cases} \alpha^3\dfrac{d^3}{dx^3}\Psi(\alpha x)+\dfrac{2\alpha^2k}{x}\dfrac{d^2}{dx^2}\Psi(\alpha x)\\ \quad+\dfrac{\alpha k(k-1)}{x^2}\dfrac{d}{dx}\Psi(\alpha x)+\Psi^\nu(x)=g(x),\\ \Psi(0)=A_1,\\ \dfrac{d\Psi(0)}{dx}=0,\\ \dfrac{d^2\Psi(0)}{dx^2}=0. \end{cases} \tag{8}$$

The singularity is performed twice at $x=0$ and $x^2=0$ while the pantographs are noticed in the first, second, and third terms. Moreover, the shape factors are $2k$ and $k(k-1)$. It is noticed for $k=1$, the third term vanishes, and the value of the shape factor becomes 2.

Category 2: the restructured form of the (2) using the (5) becomes as

$$x^{-k}\frac{d}{dx}\left(x^k\frac{d^2}{dx^2}\Psi(\alpha x)\right)+\Psi^\nu(x)=g(x). \tag{9}$$

By calculating the derivative, the obtained form is given as

$$\begin{aligned} \frac{d}{dx}\left(x^k\frac{d^2}{dx^2}\Psi(\alpha x)\right)&=\alpha^3x^k\frac{d^3}{dx^3}\Psi(\alpha x)\\ &\quad+\alpha^2kx^{k-1}\frac{d^2}{dx^2}\Psi(\alpha x). \end{aligned} \tag{10}$$

Using (10) in (2), the nonlinear third-order PD-LE model is given as

$$\begin{cases} \alpha^3 \dfrac{d^3}{dx^3}\Psi(\alpha x) + \dfrac{\alpha^2 k}{x}\dfrac{d^2}{dx^2}\Psi(\alpha x) + \Psi^{\nu}(x) = g(x), \\ \Psi(0) = A_1, \\ \dfrac{d\Psi(0)}{dx} = A_2, \\ \dfrac{d^2\Psi(0)}{dx^2} = 0. \end{cases} \tag{11}$$

The single singularity appears at zero in (11). k is the shape factor, and pantograph expressions appear twice in (11).

3. Fundamental Relationships/ Function Calculation

This section states the basic Bernoulli polynomials (BPs) properties. BPs play a significant role in the fields of mathematics, including finite difference theory and the integral representations of the periodic function. BPs are the type of nonorthogonal polynomials, and their basic definitions are found in references [59]. The classical form of the BPs is given as

$$\begin{aligned} \frac{te^{\eta t}}{e^t - 1} &= \sum_{k=0}^{n} B_k(x)\frac{t^k}{k!}, \\ \sum_{k=0}^{n}\binom{n+1}{k}B_k(x) &= (n+1)x^n. \end{aligned} \tag{12}$$

These above polynomials designate the various properties, such as,

$$\begin{aligned} B_n'(x) &= nB_{n-1}(x), \quad n \geq 1, \\ \int_0^1 B_n(x)dx &= -\left(\frac{B_{n+1}(0) - B_{n+1}(1)}{n+1}\right), \\ B_n(x+1) &= nx^{n-1} + B_n(x). \end{aligned} \tag{13}$$

BPs have many advantages/merits, and the execution of the Bernoulli operational matrix approach is quite easy. One of the main advantages of the BPs is that the operational differential matrix has fewer nonzero elements than other polynomials. The first subdiagonal elements are nonzero in Bernoulli's operational matrix of its derivative, and the coefficient values of the individual terms in Bernoulli polynomials are much smaller than the coefficients, which appear in the classical orthogonal polynomials to produce fewer computational errors. Due to the wide range of applications as well as the advantages of the BPs, this method is reliable to be implemented as compared to other approaches.

3.1. Differential Form of the Bernoulli Operational Matrix. BPs have various interesting properties and relations, including the derivative to solve different categories of problems. The approximation form of the Bernoulli approximation scheme is expressed as

$$\begin{aligned} \Psi_N(x) &= \sum_{i=0}^{N} c_i B_i(x) \\ &= B(x)\mathbf{C}, \end{aligned} \tag{14}$$

where $\{c_i\}_{i=0}^N$ is the unidentified coefficient values, N is a positive integer taken as $N \geq 2$, and $B_i(x)$ is the BP of the first kind, which can be formulated according to (12) in the following form as

$$\underbrace{\begin{bmatrix} B_0(x) \\ B_1(x) \\ \vdots \\ B_N(x) \end{bmatrix}}_{B^T(x)} = \underbrace{\begin{bmatrix} B_0(0) & 0 & \cdots & 0 \\ \binom{1}{1}B_1(0) & \binom{1}{0}B_0(0) & \cdots & 0 \\ \binom{2}{2}B_2(0) & \binom{2}{1}B_{11}(0) & \cdots & 0 \\ \vdots & \vdots & \ddots & \vdots \\ \binom{N}{N}B_N(0) & \binom{N}{N-1}B_{N-1}(0) & \cdots & \binom{N}{0}B_0(0) \end{bmatrix}}_{D} \underbrace{\begin{bmatrix} 1 \\ x \\ \vdots \\ x^N \end{bmatrix}}_{\rho^T(x)}, \tag{15}$$

where D is the lower triangle matrix having nonzero diagonal elements with $\det(D) = 1$. It can be considered as an invertible matrix, and the Bernoulli vector takes the form as

$$B(x) = \rho(x)D^T, \tag{16}$$

where $\rho(x)$ and $B(x)$ be the $(N+1) \times 1$, while D is $(N+1) \times (N+1)$ matrix which is given as

$$\{D\}_{i,j=1}^{N+1} = \begin{cases} \begin{pmatrix} i-1 \\ j-1 \end{pmatrix} \mathbf{B}_{i-j}, & i \geq j, \\ 0, & i < j. \end{cases} \quad (17)$$

Additionally, both the coefficient vectors $\mathbf{c}$ and the polynomial $\mathbf{B}(\mathbf{x})$ are written as

$$\begin{aligned} \mathbf{C}^T &= [c_0, c_1, c_2, \ldots, c_N], \\ \mathbf{B}(x) &= [B_0, B_1, B_2, \ldots, B_N]. \end{aligned} \quad (18)$$

Consider the solution form (14) is written in the following form:

$$\Psi(x) = \rho(x) D^T c. \quad (19)$$

According to (16), the relationship between $\rho(x)$ and its derivative $\rho^{(1)}(x)$ is written as

$$\rho^{(1)}(x) = \underbrace{\left[1, x, x^2, \ldots, x^N\right]}_{\mathbf{M}} \underbrace{\begin{bmatrix} 0 & 1 & 0 & 0 & \cdots & 0 \\ 0 & 0 & 2 & 0 & \cdots & 0 \\ 0 & 0 & 0 & 3 & \cdots & 0 \\ \cdots & \cdots & \cdots & \cdots & \ddots & \cdots \\ 0 & 0 & 0 & 0 & 0 & N \\ 0 & 0 & 0 & 0 & 0 & 0 \end{bmatrix}}_{\mathbf{M}}, \quad (20)$$

where M is an operational matrix based on the BPs differentiation, and the i^{th} derivative equation can take the following form:

$$\begin{aligned} \rho^{(i)}(x) &= \rho(x) \mathbf{M}^k, k \\ &= 1, 2, 3, \ldots \end{aligned} \quad (21)$$

Finally, the solution derivative takes the following form:

$$\begin{aligned} \Psi_N^{(k)}(x) &= B(x) \mathbf{M}^k \mathbf{C} \\ &= \rho(x) \mathbf{M}^k \mathbf{D}^T \mathbf{C}, k \\ &= 0, 1, 2, 3. \end{aligned} \quad (22)$$

The approximate outcomes are signified in the (19) and (22) to operate the approximate results of the given system.

3.2. Bernoulli Matrix Approach. The proposed BPs are used to solve both types represented in the system (8) and (11), respectively. The method begins with the approximate outcomes using the BPs, given as

$$\begin{aligned} \Psi_N(x) &= \sum_{n=0}^{N} c_n B_n(x) \\ &= B(x) \mathbf{C}. \end{aligned} \quad (23)$$

For the above system, the k^{th} derivative takes the following form:

$$\begin{aligned} \Psi_N^{(k)}(x) &= B(x) \mathbf{M}^k \mathbf{C}, k \\ &= 0, 1, 2, 3. \end{aligned} \quad (24)$$

Category 1: Our primary focus here is to examine category 1 represented by (8). To overcome the singularity in the system (8), the main equation is transformed into regular ones using the L'Hopital rule [60, 61] based on the expression $\Psi''(\alpha x)/x$ into the system (8), since $x = 0$ as

$$\lim_{x \longrightarrow 0} \frac{2\alpha^2 k}{x} \Psi''(\alpha x) = \frac{\Psi''(0)}{0} = \frac{0}{0}, \quad (25)$$

and hence,

$$\lim_{x \longrightarrow 0} \frac{2\alpha^2 k}{1} \Psi'''(\alpha x) = \frac{2\alpha^2 k \Psi'''(0)}{1} = 2\alpha^2 k \Psi'''(0), \quad (26)$$

and for the second expression $\Psi'(\alpha x)/x^2$, the L'Hopital rule is applied, which will transform into

$$\lim_{x \longrightarrow 0} \frac{\alpha k(k-1)}{x^2} \Psi'(\alpha x) = \frac{\Psi'(0)}{0} = \frac{0}{0}, \quad (27)$$

and hence,

$$\begin{aligned} \lim_{x \longrightarrow 0} \frac{\alpha k(k-1)}{2\text{x}} \Psi''(\alpha x) &= \lim_{x \longrightarrow 0} \frac{\alpha k(k-1)}{2} \Psi'''(\alpha x) \\ &= \frac{\alpha k(k-1)}{2} \Psi'''(0). \end{aligned} \quad (28)$$

Equation (8) will be reduced to the following form:

$$\begin{aligned} &\alpha^3 \frac{d^3}{dx^3} \Psi(\alpha x) + \mathscr{M}_1 \frac{d^2}{dx^2} \Psi(\alpha x) + \mathscr{M}_2 \frac{d}{dx} \Psi(\alpha x) \\ &\quad + \frac{1}{\mathfrak{R}} \Psi^{\nu}(x) = \wp(x), \end{aligned} \quad (29)$$

where

$$\begin{aligned} \mathscr{M}_1 &= \begin{cases} \dfrac{1}{\mathfrak{R}}, & x = 0, \\ \dfrac{2\alpha^2}{x}, & x \neq 0, \end{cases} \\ \mathscr{M}_2 &= \begin{cases} \dfrac{1}{\mathfrak{R}}, & x = 0, \\ \dfrac{\alpha k(k-1)}{x^2}, & x \neq 0, \end{cases} \\ \wp(x) &= \begin{cases} \dfrac{g(0)}{\mathfrak{R}}, & x = 0, \\ g(x), & x \neq 0, \end{cases} \end{aligned} \quad (30)$$

and $\mathfrak{R} = \alpha^3 + 2\alpha^2 + \alpha k(k-1)/2$. Thus, the double singularity will be handled here using the previous transformation.

Next, we substitute the solution and its approximation from the (17) and (18) as

$$\alpha^3 \sum_{n=0}^{N} B(\alpha x)\mathbf{M}^3\mathbf{C} + \mathscr{M}_1 \sum_{n=0}^{N} B(\alpha x)\mathbf{M}^2\mathbf{C} + \mathscr{M}_2 \sum_{n=0}^{N} B(\alpha x)\mathbf{M}\mathbf{C} + \frac{1}{\mathfrak{R}}\Psi^{\upsilon}(x) = \wp(x), \tag{31}$$

where any function except $\Psi^{\nu}(x)$ will be extended by using any appropriate expansion. To solve the equation (31) using the adjustable collocation points is given as

$$x_j = \frac{1}{N} j, \quad j = 0, 1, 2, \ldots, N. \tag{32}$$

By substituting these collocation points into (31), one can find as

$$\alpha^3 \sum_{n=0}^{N} B(\alpha x_j)\mathbf{M}^3\mathbf{C} + \mathscr{M}_1 \sum_{n=0}^{N} B(\alpha x_j)\mathbf{M}^2\mathbf{C} + \mathscr{M}_2 \sum_{n=0}^{N} B(\alpha x_j)\mathbf{M}\mathbf{C} + \frac{1}{\mathfrak{R}}\Psi^{\upsilon}(x_j) = \wp(x_j). \tag{33}$$

To solve the above equation, it is essential to handle the nonlinear term $\Psi^{\nu}(x)$ stated in the theorem.

Theorem 1. *The approximation of the function $\Psi^{\nu}(x_j)$, $j = 0, 1, 2, \ldots, N$ can be performed according to the next relation as*

$$\begin{pmatrix} \Psi^{\nu}(x_0) \\ \Psi^{\nu}(x_1) \\ \vdots \\ \Psi^{\nu}(x_N) \end{pmatrix} = \begin{pmatrix} \Psi(x_0) & 0 & \cdots & 0 \\ 0 & \Psi(x_1) & \cdots & 0 \\ \vdots & \vdots & \ddots & \vdots \\ 0 & 0 & \cdots & \Psi(x_n) \end{pmatrix}^{\nu-1} \begin{pmatrix} \Psi^{\nu}(x_0) \\ \Psi^{\nu}(x_1) \\ \vdots \\ \Psi^{\nu}(x_N) \end{pmatrix} = (I)^{n-1} I = (\widetilde{\mathbf{B}}\widetilde{\mathbf{C}})^{n-1} (\mathbf{BC}), \tag{34}$$

where

$$\widetilde{\mathbf{B}} = \begin{pmatrix} B(x_0) & 0 & \cdots & 0 \\ 0 & B(x_1) & \cdots & 0 \\ \vdots & \vdots & \ddots & \vdots \\ 0 & 0 & \cdots & B(x_N) \end{pmatrix}, \quad \widetilde{\mathbf{C}} = \begin{pmatrix} \mathbf{c} & 0 & \cdots & 0 \\ 0 & \mathbf{c} & \cdots & 0 \\ \vdots & \vdots & \ddots & \vdots \\ 0 & 0 & \cdots & \mathbf{c} \end{pmatrix}, \quad \mathbf{B} = \begin{pmatrix} B_0(x_0) & B_1(x_0) & \ldots & B_N(x_0) \\ B_0(x_1) & B_1(x_1) & \ldots & B_N(x_1) \\ B_0(x_2) & B_1(x_2) & \ldots & B_N(x_2) \\ \vdots & \vdots & \vdots & \vdots \\ B_0(x_N) & B_1(x_N) & \ldots & B_N(x_N) \end{pmatrix}. \tag{35}$$

Proof. The proof can be found in [62].

Next, by substituting $x = x_j$ in equation (32) and approximate values using equations (20) and (23), the following theorem is obtained. □

Theorem 2. *If the assumed approximate solution to the problem (8) is represented by (19) and (22), then the discrete form of the Bernoulli system can be given in the following form:*

$$\alpha^3 \sum_{n=0}^{N} B(\alpha x_j)\mathbf{M}^3\mathbf{C} + \mathscr{M}_1 \sum_{n=0}^{N} B(\alpha x_j)\mathbf{M}^2\mathbf{C} + \mathscr{M}_2 \sum_{n=0}^{N} B(\alpha x_j)\mathbf{M}\mathbf{C} + \frac{1}{\mathfrak{R}}\Psi^{\upsilon}(x_j) = \wp(x_j). \tag{36}$$

Proof. If we replace each term of (8) with its corresponding approximation given by equations (20)–(23) and by substituting $x = x_k$ collocation points defined previously, (33) can be written in matrix form as

$$\mathbf{\Theta}\mathbf{C} = \mathscr{H}, \tag{37}$$

where $\Theta = \alpha^3\widehat{\mathbf{B}}\mathbf{M}^3 + \mathscr{M}_1\widehat{\mathbf{B}}\mathbf{M}^2 + \mathscr{M}_2\widehat{\mathbf{B}}\mathbf{M} + \ell(\widetilde{\mathbf{B}}\widetilde{\mathbf{C}})^{n-1}(\mathbf{BC})$ and

$$\widehat{\mathbf{B}} = \begin{pmatrix} B_0(\alpha x_0) & B_1(\alpha x_0) & \dots & B_N(\alpha x_0) \\ B_0(\alpha x_1) & B_1(\alpha x_1) & \dots & B_N(\alpha x_1) \\ B_0(\alpha x_2) & B_1(\alpha x_2) & \dots & B_N(\alpha x_2) \\ \vdots & \vdots & \vdots & \vdots \\ B_0(\alpha x_N) & B_1(\alpha x_N) & \dots & B_N(\alpha x_N) \end{pmatrix},$$

$$\mathscr{M}_1 = \begin{pmatrix} \frac{2\alpha^2 k}{x_0} & 0 & \cdots & 0 \\ 0 & \frac{2\alpha^2 k}{x_1} & \cdots & 0 \\ \vdots & \vdots & \ddots & \vdots \\ 0 & 0 & \cdots & \frac{2\alpha^2 k}{x_N} \end{pmatrix},$$

$$\mathscr{M}_2 = \begin{pmatrix} \frac{\alpha k(k-1)}{x_0^2} & 0 & \cdots & 0 \\ 0 & \frac{\alpha k(k-1)}{x_1^2} & \cdots & 0 \\ \vdots & \vdots & \ddots & \vdots \\ 0 & 0 & \cdots & \frac{\alpha k(k-1)}{x_N^2} \end{pmatrix}, \tag{38}$$

$$\ell = \begin{pmatrix} \frac{1}{\mathfrak{R}} & 0 & \cdots & 0 \\ 0 & \frac{1}{\mathfrak{R}} & \cdots & 0 \\ \vdots & \vdots & \ddots & \vdots \\ 0 & 0 & \cdots & \frac{1}{\mathfrak{R}} \end{pmatrix},$$

$$\mathscr{H} = \begin{pmatrix} g(x_0) \\ g(x_1) \\ \vdots \\ g(x_N) \end{pmatrix}.$$

It is noted that the matrix $\widehat{\mathbf{B}}$ is used for the delayed terms. The technique applications of the differential form of model (8) are converted into a matrix equation that corresponds to $N+1$ linear algebraic system in $N+1$ unknown value of Bernoulli coefficients. The improved matrix form becomes as

$$[\boldsymbol{\Theta}; \mathscr{H}] = \begin{pmatrix} \Theta_{00} & \Theta_{01} & \cdots & \Theta_{0N} & \vdots & g(x_0) \\ \Theta_{10} & \Theta_{11} & \cdots & \Theta_{1N} & \vdots & g(x_1) \\ \Theta_{20} & \Theta_{21} & \cdots & \Theta_{2N} & \vdots & \vdots \\ \vdots & \vdots & \cdots & \vdots & \vdots & \vdots \\ \Theta_{N0} & \Theta_{N1} & \cdots & \Theta_{NN} & \vdots & g(x_N) \end{pmatrix}. \tag{39}$$

The initial form of system (8) is provided using the matrix form

$$\begin{aligned} B(0)c &= A_1, \text{ or } U_{1,i}c = A_1 \\ B(0)Mc &= 0, \text{ or } U_{2,i}c = 0, \\ B(0)M^2c &= 0, \text{ or } U_{3,i}c = 0, \quad i = 0, 1, 2, \dots, N. \end{aligned} \tag{40}$$

Finally, the corresponding rows are replaced with the initial conditions represented in (36) with the augmented matrix form of (35), which shall result in a new augmented form as

$$\begin{aligned} \widetilde{\boldsymbol{\Theta}}\,\mathbf{C} &= \widetilde{\mathscr{H}}\,[\widetilde{\boldsymbol{\Theta}}; \widetilde{\mathscr{H}}] \\ &= \begin{pmatrix} U_{1,0} & U_{1,1} & \cdots & U_{1,N} & \vdots & A_1 \\ U_{2,0} & U_{2,1} & \cdots & U_{2,N} & \vdots & 0 \\ \Theta_{20} & \Theta_{21} & \cdots & \Theta_{2N} & \vdots & 0 \\ \vdots & \vdots & \cdots & \vdots & \vdots & \vdots \\ \Theta N_0 & \Theta_{N1} & \cdots & \Theta_{NN} & \vdots & 0 \end{pmatrix}. \end{aligned} \tag{41}$$

The unknown coefficients **C** can be calculated by applying the next algorithm [50].

Category 2: Here, category (2) is examined for equation (11) using the same previously introduced technique which is applied to equation (11), and thus, the approximation from equations (18) and (19) along with Theorem 1 will reach the following theorem. □

Theorem 3. *If the assumed approximate solutions to the problem (11) are equations (17)–(19), then the discrete form of the Bernoulli system can be given in the following form:*

$$\begin{aligned} \alpha^3 \sum_{n=0}^{N} B(\alpha x_j)\mathbf{M}^3\mathbf{C} + \mathscr{M}_1 \sum_{n=0}^{N} B(\alpha x_j)\mathbf{M}^2\mathbf{C} \\ + \frac{1}{\mathfrak{R}}\Psi^{v}(x_j) = \wp(x_j). \end{aligned} \tag{42}$$

Proof. If each term of (11) is replaced with its corresponding approximations given in equations (17)–(19), and substituting $x = x_k$, which is the collocation points defined previously, (39) can be written in matrix form as

$$\mathbb{Z}\,\mathbf{C} = \mathscr{H}, \tag{43}$$

where $\mathbb{Z} = \alpha^3\widehat{\mathbf{B}}\mathbf{M}^3 + \mathscr{M}_1\widehat{\mathbf{B}}\mathbf{M}^2 + \ell(\widetilde{\mathbf{B}}\widetilde{\mathbf{C}})^{n-1}(\mathbf{BC})$, where $\widehat{B}$, $\widetilde{B}$, $\widetilde{C}$, $\mathscr{M}_1$, $\mathscr{M}_2$, and ℓ have been defined previously after

(i) Input form of the integer N.
(ii) input (double) tol.
(iii) Input (array) $c_{\text{old}} = c_0$ (initial guess, c_0 with $N + 1$ dimension can be selected to satisfy the boundary conditions)
(iv) $\widetilde{\Theta}(c_{\text{old}})c_{\text{new}} = \widetilde{\mathbf{F}}$, is an algebraic linear system and c^{*}_{new} is achieved.
(v) If $|c_{\text{old}} - c_{\text{new}}| < tol$ then $c_{\text{new}} = c$, (the program is terminated).
(vi) Else $c_{\text{old}} \leftarrow c_{\text{new}}$.

Algorithm 1: Algorithm.

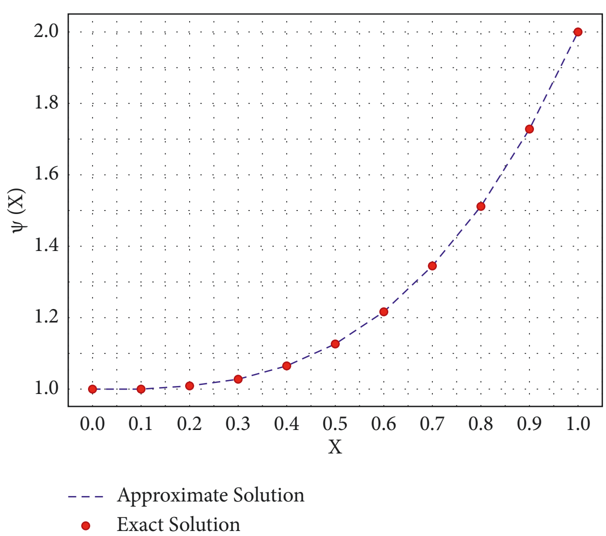

Figure 1: Proposed and exact solutions for Problem 1 at $N = 6$.

Table 1: Absolute error for Problem 1.

x_i	$\lvert e_6(x_i)\rvert$	$\lvert e_8(x_i)\rvert$	$\lvert e_{10}(x_i)\rvert$
0.0	0	$2.3214e-16$	0
0.1	$1.9984e-15$	$3.4510e-16$	$2.3214e-16$
0.2	$9.1038e-15$	$1.3323e-15$	$4.4409e-16$
0.3	$1.8652e-14$	$2.2204e-15$	$6.6613e-16$
0.4	$2.7311e-14$	$2.6645e-15$	$6.6613e-16$
0.5	$3.4417e-14$	$3.3307e-15$	$8.8818e-16$
0.6	$3.3973e-14$	$5.1070e-15$	$4.4409e-16$
0.7	$1.9984e-15$	$1.8874e-14$	$8.8818e-16$
0.8	$1.4833e-13$	$8.3267e-14$	$1.7319e-14$
0.9	$5.6244e-13$	$2.9954e-13$	$1.1324e-13$
1.0	$1.5268e-12$	$8.8507e-13$	$4.5164e-13$

(34). The conditions for category 2 are in the same form as (36).

$$\begin{aligned} B(0)c &= A_1, \text{ or } U_{1,i}c = A_1 \\ B(0)Mc &= A_2, \text{ or } U_{2,i}c = A_2, \\ B(0)M^2c &= 0, \text{ or } U_{3,i}c = 0, \quad i = 0, 1, 2, \ldots, N. \end{aligned} \tag{44}$$

Finally, the new augmented matrix for system (37) which can take the following form after replacing the conditions in equation (38) with the defined conditions in equation (39) is written as

Table 2: Residual error for Problem 1.

x_i	$\lvert\vartheta_6(x_i)\rvert$	$\lvert\vartheta_8(x_i)\rvert$	$\lvert\vartheta_{10}(x_i)\rvert$
0.1	$7.6851e-12$	$1.1710e-12$	$6.1314e-13$
0.2	$4.0604e-12$	$3.9074e-13$	$8.5103e-14$
0.3	$1.7799e-12$	$7.2622e-14$	$1.0476e-15$
0.4	$5.4362e-13$	$5.6212e-15$	$2.8460e-16$
0.5	$4.9830e-14$	$1.6108e-15$	$1.2574e-17$
0.6	$1.1279e-14$	$6.6948e-15$	$2.0688e-16$
0.7	$3.5697e-16$	$6.7570e-15$	$6.9272e-16$
0.8	$4.5662e-13$	$1.5609e-13$	$2.5614e-14$
0.9	$2.4153e-12$	$9.8761e-13$	$3.0835e-13$
1.0	$8.1086e-12$	$3.9903e-12$	$1.7364e-12$

$$\begin{gathered} \widetilde{\mathbb{Z}}\,\mathbf{C} = \widetilde{\mathscr{H}}, \\ [\widetilde{\mathbb{Z}}; \widetilde{\mathscr{H}}] = \begin{pmatrix} U_{1,0} & U_{1,1} & \cdots & U_{1,N} & \vdots & A_1 \\ U_{2,0} & U_{2,1} & \cdots & U_{2,N} & \vdots & A_2 \\ \mathbb{Z}_{20} & \mathbb{Z}_{21} & \cdots & \mathbb{Z}_{2N} & \vdots & 0 \\ \vdots & \vdots & \cdots & \vdots & \vdots & \vdots \\ \mathbb{Z}_{N_0} & \mathbb{Z}_{N1} & \cdots & \mathbb{Z}_{NN} & \vdots & 0 \end{pmatrix}. \end{gathered} \tag{45}$$

Then, the new system in (39) shall be solved using the same previously mentioned algorithm to find the unknown coefficients. In the next section, the verification of the residual error function is presented to confirm the validity of the proposed technique. □

4. Residual Error Function

The solution accuracy for category I represented by equation (8) and the same for category II based on the residual error function are observed in this section as

$$\begin{aligned} \vartheta(x_j) = \Bigg| &\alpha^3 \frac{d^3}{dx^3}\Psi(\alpha x) + \frac{2\alpha^2 k}{x}\frac{d^2}{dx^2}\Psi(\alpha x) \\ &+ \frac{\alpha k(k-1)}{x^2}\frac{d}{dx}\Psi(\alpha x) + h(\Psi) - g(x)\Bigg| \cong 0, \end{aligned} \tag{46}$$

or $\vartheta(\eta_j) \le 10^{-\tau_j}$, τ_j (positive) for $\eta_j \in [a, b]$, $j = 0, 1, 2, \ldots$.

The proposed technique must be tested for the numerical solutions based on the (8) and (11). The max $10^{-\tau_j}$ is defined for the truncated limit N and is then improved till the $\vartheta(\eta_j)$ variation becomes smaller at each point than the maximum $10^{-\tau_j}$. Calculating the residual error represented by (40) will ensure the effectivity of the proposed algorithm along with calculating the regular absolute error.

Table 3: Comparison of exact and approximate solutions for Problem 2.

x_i	Exact solution $\Psi(x_i)$	Proposed method $\Psi_6(x_i)$	$\Psi_8(x_i)$	$\Psi_{10}(x_i)$
0.0	1.000000000000000	1.000000000000000	1.000000000000000	1.000000000000000
0.1	1.001105170918076	1.001091993998999	1.001105107494984	1.001105170789825
0.2	1.009771222065281	1.009708020730964	1.009770993250848	1.009771221695879
0.3	1.036446187804552	1.036319546728776	1.036445805625290	1.036446187246225
0.4	1.095476780649041	1.095294402016241	1.095476279954487	1.095476779951982
0.5	1.206090158837516	1.205863263540755	1.206089570316998	1.206090158070000
0.6	1.393577660884350	1.393324172349599	1.393576972058984	1.393577660157947
0.7	1.690717178662373	1.690485084509886	1.690716376006776	1.690717177586527
0.8	2.139476955388143	2.139344455772156	2.139476444262095	2.139476952381585
0.9	2.793050668033416	2.793009859977607	2.793051646444440	2.793050663451304
1.0	3.718281828459045	3.717854641208983	3.718283444214394	3.718281825935696

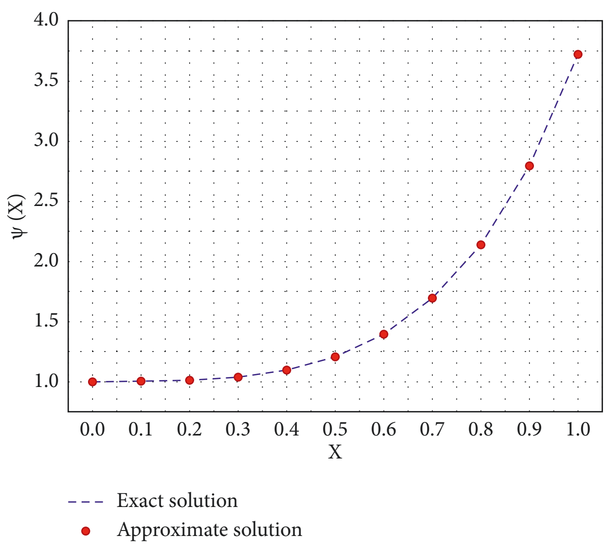

Figure 2: Proposed and exact solutions for Problem 2 at $N = 6$.

Table 4: Absolute error for Problem 2.

x_i	$\lvert e_6(x)\rvert$	$\lvert e_8(x)\rvert$	$\lvert e_{10}(x)\rvert$
0.0	$1.1102e-16$	0	0
0.1	$1.3177e-05$	$6.3423e-08$	$1.2825e-10$
0.2	$6.3201e-05$	$2.2881e-07$	$3.6940e-10$
0.3	$1.2664e-04$	$3.8218e-07$	$5.5833e-10$
0.4	$1.8238e-04$	$5.0069e-07$	$6.9706e-10$
0.5	$2.2690e-04$	$5.8852e-07$	$7.6752e-10$
0.6	$2.5349e-04$	$6.8883e-07$	$7.2640e-10$
0.7	$2.3209e-04$	$8.0266e-07$	$1.0758e-09$
0.8	$1.3250e-04$	$5.1113e-07$	$3.0066e-09$
0.9	$4.0808e-05$	$9.7841e-07$	$4.5821e-09$
1.0	$4.2719e-04$	$1.6158e-06$	$2.5233e-09$

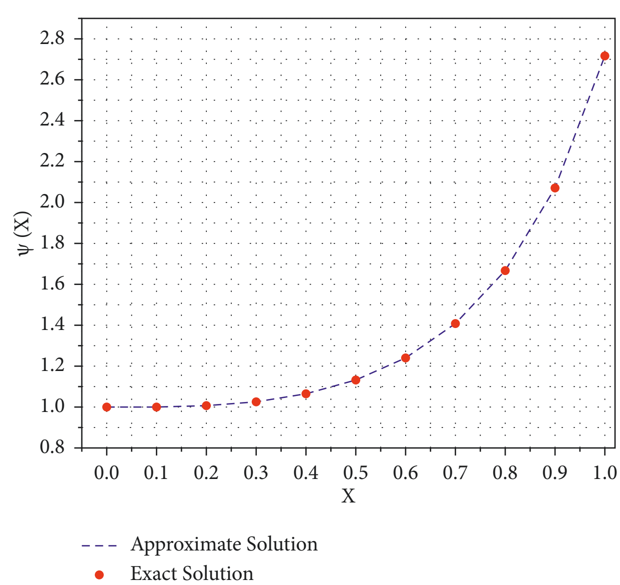

Figure 3: : Approximate and exact solutions for Problem 3.

In the next section, we shall test the proposed method for several nonlinear examples to verify its effectiveness.

5. Numerical Results

In this section, four different numerical variants are accomplished to check the exactness and perfection based on the nonlinear PD-LE model along with the efficiency and accuracy of the Bernoulli collocation scheme. The absolute error (AE) is calculated from the proposed solutions based on the BC scheme, and the true results are provided at the selected points. All the computations have been performed in MATLAB R2015a. No MATLAB built-in syntax has been used while preparing the coding of the examples. Also, the tolerance for the prosed scheme in all the examples is assigned to be 10^{-10}.

5.1. PD-LE Model of Category 1. In this category, two different equations of PD-LE third-order model-based examples will be presented. The simplified form of (8) for $k=2$ is written as shown in the following problem.

Table 5: Comparison of absolute error for Problem 3.

x_i	$\lvert e(x)\rvert$	Neuro-swarming-based heuristics technique [63]	Intelligent computing paradigm [64]
0.0	**5.2292e – 13**	2.0*e* – 04	2.8*e* – 01
0.1	**2.3959e – 07**	1.7*e* – 04	2.9*e* – 01
0.2	**6.2978e – 07**	1.7*e* – 04	3.4*e* – 01
0.3	**9.3909e – 07**	1.7*e* – 04	3.8*e* – 01
0.4	**1.1981e – 06**	1.6*e* – 04	4.2*e* – 01
0.5	**1.4434e – 06**	1.8*e* – 04	4.7*e* – 01
0.6	**1.7081e – 06**	2.2*e* – 04	5.3*e* – 01
0.7	**2.0307e – 06**	2.5*e* – 04	6.2*e* – 01
0.8	**2.4652e – 06**	3.3*e* – 04	7.4*e* – 01
0.9	**3.0976e – 06**	3.7*e* – 04	9.3*e* – 01
1.0	**4.0768e – 06**	5.2*e* – 04	1.2*e* + 00

Table 6: Absolute error for Problem 4.

x_i	$\lvert e_6(x_i)\rvert$	$\lvert e_8(x_i)\rvert$	$\lvert e_{10}(x_i)\rvert$	$\lvert e_{12}(x_i)\rvert$
0.0	0	0	0	0
0.1	7.6976*e* – 08	1.7732*e* – 10	2.3137*e* – 13	6.6613*e* – 16
0.2	4.3224*e* – 07	8.3860*e* – 10	9.6101*e* – 13	2.4425*e* – 15
0.3	1.0321*e* – 06	1.8035*e* – 09	1.9447*e* – 12	4.8850*e* – 15
0.4	1.7544*e* – 06	2.8872*e* – 09	3.0120*e* – 12	7.3275*e* – 15
0.5	2.4876*e* – 06	3.9381*e* – 09	4.0079*e* – 12	9.7700*e* – 15
0.6	3.1246*e* – 06	4.8553*e* – 09	4.7793*e* – 12	1.2212*e* – 14
0.7	3.5436*e* – 06	5.5334*e* – 09	5.4770*e* – 12	1.3989*e* – 14
0.8	3.6679*e* – 06	5.5495*e* – 09	6.7280*e* – 12	4.2188*e* – 15
0.9	3.6870*e* – 06	4.1718*e* – 09	7.8142*e* – 12	4.7740*e* – 14
1.0	4.5206*e* – 06	2.8842*e* – 09	6.0032*e* – 12	2.0761*e* – 13
CPU time	**1.40**	**1.78**	**2.60**	**14.50**

Problem 1. Consider the following nonlinear PD-LE model:

$$\begin{cases} \dfrac{1}{8}\dfrac{d^3}{dx^3}\Psi\left(\dfrac{x}{2}\right)+\dfrac{1}{x}\dfrac{d^2}{dx^2}\Psi\left(\dfrac{x}{2}\right)+\dfrac{1}{x^2}\dfrac{d}{dx}\Psi\left(\dfrac{x}{2}\right) \\ \quad +x\Psi^2 = x^7+2x^4+x+\dfrac{9}{2}, \\ \Psi(0)=1, \\ \dfrac{d\Psi(0)}{dx}=0, \\ \dfrac{d^2\Psi(0)}{dx^2}=0. \end{cases} \tag{47}$$

The exact solution of (37) is $\Psi(x)=1+x^3$. The numerical results to express the maximum AE are provided in Table 1 for different values of N. It can be found from this table that the method provides accurate solutions in terms of the absolute error with an error of 10^{-16}, and the CPU time is 5.8 sec. Also, the proposed technique is witnessed to achieve high accuracy results even for a little number of bases. In addition, Figure 1 gives the approximate and exact solution for (31) with $N=6$. It can be noticed from the figures that the resulting approximate solution fits well with the exact results proving the method is efficient. Also, to confirm the validity of the proposed technique, the results of the residual error are illustrated in Table 2.

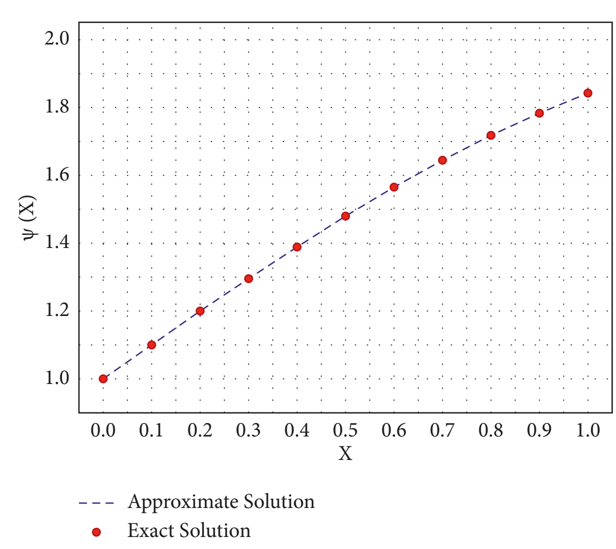

Figure 4: Approximate and exact solutions for Problem 4.

Problem 2. Consider the third-order nonlinear PD-LE model involving exponential values in the forcing factor, that is,

Table 7: Residual error for Problem 4.

x_i	$\lvert\vartheta_6(x_i)\rvert$	$\lvert\vartheta_8(x_i)\rvert$	$\lvert\vartheta_{10}(x_i)\rvert$
0.1	$3.6137e-05$	$4.7518e-08$	$1.6679e-11$
0.2	$9.3493e-06$	$1.6304e-08$	$4.1251e-11$
0.3	$3.7598e-06$	$2.4593e-08$	$2.7190e-11$
0.4	$7.9224e-06$	$1.6044e-08$	$1.2836e-11$
0.5	$6.9268e-06$	$7.4968e-09$	$5.9737e-12$
0.6	$3.7787e-06$	$3.0285e-09$	$2.2237e-12$
0.7	$8.6139e-07$	$8.7238e-10$	$2.0952e-13$
0.8	$2.0032e-07$	$6.9998e-10$	$6.6338e-13$
0.9	$6.4822e-07$	$9.1559e-11$	$3.7974e-13$
1.0	$4.6153e-12$	$3.2264e-12$	$1.7771e-12$

Table 8: Comparison of exact and proposed solutions for Problem 5.

	Exact solution		Proposed method	
x_i	$\Psi(x_i)$	$\Psi_6(x_i)$	$\Psi_8(x_i)$	$\Psi_{10}(x_i)$
0.0	1.000000000000000	1.000000000000000	1.000000000000000	1.000000000000000
0.1	1.106170918075648	1.106170785680663	1.106170917762990	1.106170918075230
0.2	1.229402758160170	1.229402004971852	1.229402756673175	1.229402758158428
0.3	1.376858807576003	1.376856997249711	1.376858804375231	1.376858807572478
0.4	1.555824697641270	1.555821627025820	1.555824692543696	1.555824697635839
0.5	1.773721270700128	1.773716971527389	1.773721263856625	1.773721270693004
0.6	2.038118800390509	2.038113537675213	2.038118792203891	2.038118800382295
0.7	2.356752707470477	2.356747008459377	2.356752698486671	2.356752707461768
0.8	2.737540928492467	2.737535518712722	2.737540919744006	2.737540928482930
0.9	3.188603111156950	3.188598460282066	3.188603104721681	3.188603111146713
1.0	3.718281828459045	3.718276816597190	3.718281824378029	3.718281828450404

$$\begin{cases} \dfrac{1}{8}\dfrac{d^3}{dx^3}\Psi\left(\dfrac{x}{2}\right)+\dfrac{1}{x}\dfrac{d^2}{dx^2}\Psi\left(\dfrac{x}{2}\right)+\dfrac{1}{x^2}\dfrac{d}{dx}\Psi\left(\dfrac{x}{2}\right)+\Psi^2 \\ \quad =\dfrac{1}{64}x^3e^{x/2}+\dfrac{13}{32}x^2e^{x/2}+\dfrac{11}{4}xe^{x/2} \\ \quad +\dfrac{9}{2}e^{x/2}+x^6e^{2x}+2x^3e^x+1, \\ \Psi(0)=1, \dfrac{d\Psi(0)}{dx}=0, \dfrac{d^2\Psi(0)}{dx^2}=0. \end{cases} \tag{48}$$

The exact form of (42) is $1+x^3e^x$. The exact and proposed solutions are presented in Table 3 for different values of N along with the maximum AE for $N=10$ at different grid points which shows that the method is accurate with little grid points. It is noticed based on Table 4 that the BC scheme is efficient that provides few error values. In addition, Figure 2 gives the approximate versus the exact solution of the problem.

Problem 3. [63, 64] To test the effectiveness of the proposed scheme, a special case is considered of the third-order PD-LE model with variable coefficients in the form as

$$\begin{cases} \dfrac{d^3}{dx^3}\Psi(x)+\dfrac{4}{x}\dfrac{d^2}{dx^2}\Psi(x)+\dfrac{2}{x^2}\dfrac{d^2}{dx^2}\Psi(x) \\ \quad -9\left(4+10x^3+3x^6\right)=0, \\ \Psi(0)=1, \\ \dfrac{d\Psi(0)}{dx}=\dfrac{d^2\Psi(0)}{dx^2}=0. \end{cases} \tag{49}$$

The exact form of (49) is $\Psi(x)=\exp x^3$. We test the method for system (44), and the results are presented in Table 5 which demonstrated the absolute error along with a comparison with the neuro-swarming-based heuristics technique presented in [63] and the intelligent computing paradigm [64]. It can be seen from the results that our technique provides better results compared to the other method. It is worth mentioning that the time consumed for processing the results is 3.03 sec while there is no consumed time mentioned in the other compared work. In addition, Figure 3 demonstrates the approximate and exact solution for the problem.

5.2. PD-LE Model of Category 2. In this category, two different problems of PD-LE third-order systems will be

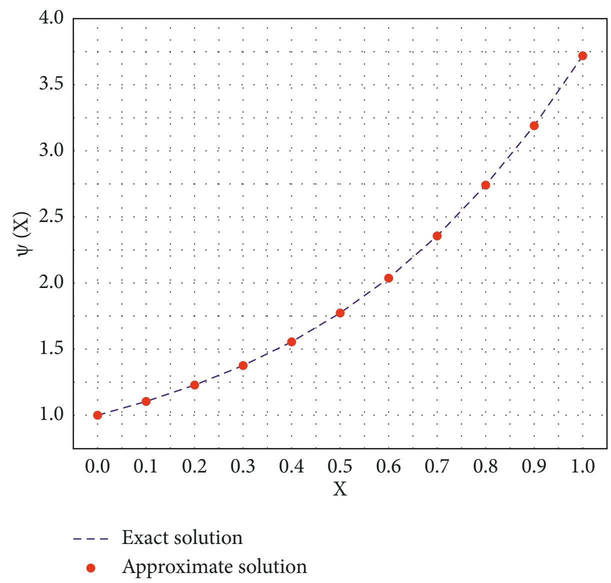

Figure 5: Proposed and exact solutions at $N = 6$ for Problem 5.

Table 9: Absolute error for Problem 5.

x_i	$\lvert e_6(x_i)\rvert$	$\lvert e_8(x_i)\rvert$	$\lvert e_{10}(x_i)\rvert$
0.0	$1.1102e-16$	0	0
0.1	$1.3239e-07$	$3.1266e-10$	$4.1744e-13$
0.2	$7.5319e-07$	$1.4870e-09$	$1.7422e-12$
0.3	$1.8103e-06$	$3.2008e-09$	$3.5256e-12$
0.4	$3.0706e-06$	$5.0976e-09$	$5.4317e-12$
0.5	$4.2992e-06$	$6.8435e-09$	$7.1243e-12$
0.6	$5.2627e-06$	$8.1866e-09$	$8.2139e-12$
0.7	$5.6990e-06$	$8.9838e-09$	$8.7086e-12$
0.8	$5.4098e-06$	$8.7485e-09$	$9.5373e-12$
0.9	$4.6509e-06$	$6.4353e-09$	$1.0237e-11$
1.0	$5.019e-06$	$4.0810e-09$	$8.6406e-12$

presented. The efficient form of equation (11) for $k=1$ is written as follows.

Problem 4. Consider the third-order nonlinear PD-LE model having multitrigonometric ratios is shown as

$$\begin{cases} \dfrac{1}{8}\dfrac{d^3}{dx^3}\Psi\left(\dfrac{x}{2}\right)+\dfrac{1}{4x}\dfrac{d^2}{dx^2}\Psi\left(\dfrac{x}{2}\right)+\Psi^2=\sin^2 x \\ \quad -\dfrac{1}{4x}\sin\left(\dfrac{x}{2}\right)+2\sin x-\dfrac{1}{8}\cos\left(\dfrac{x}{2}\right)+1, \\ \Psi(0)=1=\dfrac{d\Psi(0)}{dx}, \\ \dfrac{d^2\Psi(0)}{dx^2}=0. \end{cases} \tag{50}$$

The exact form of (44) is $\Psi(x)=1+\sin x$. The scheme is applied to the given equation along with the maximum AE provided in Table 6 for different values of N together with its maximum error of 10^{-14} for $N=12$. Also, the residual error results for N are provided in Table 7. In addition, Figure 4 gives the approximate and exact solutions for (44) with $N=6$.

Problem 5. Consider the third-order nonlinear PD-LE model having exponential values that can be presented as

$$\begin{cases} \dfrac{1}{8}\dfrac{d^3}{dx^3}\Psi\left(\dfrac{x}{2}\right)+\dfrac{1}{4x}\dfrac{d^2}{dx^2}\Psi\left(\dfrac{x}{2}\right)+\Psi^2=x^6+2x^3e^x \\ \quad +e^{2x}+\dfrac{1}{4x}e^{x/2}+\dfrac{1}{8}e^{x/2}+\dfrac{3}{2}, \\ \Psi(0)=\dfrac{d\Psi(0)}{dx}=\dfrac{d^2\Psi(0)}{dx^2}=1. \end{cases} \tag{51}$$

The exact solution of (45) is $\Psi(x)=x^3+e^x$. The exact and approximate solution in Table 8 along with the maximum AE is dissipated in Table 9 for different N values. In addition, Figure 5 gives the approximate and exact solution for (45) with $N=6$.

Table 10: Comparison of absolute error for Problem 6.

x_i	$\lvert e(x_i)\rvert$	Integrated intelligent computing paradigm [52]
0.0	$6.6613e-16$	$1.5e-10$
0.1	$3.2017e-11$	$2.9e-08$
0.2	$9.9400e-11$	$7.9e-08$
0.3	$1.7118e-10$	$6.7e-08$
0.4	$2.4442e-10$	$5.0e-08$
0.5	$3.1951e-10$	$5.3e-08$
0.6	$3.9750e-10$	$6.5e-08$
0.7	$4.7999e-10$	$6.6e-08$
0.8	$5.6926e-10$	$3.6e-08$
0.9	$6.6855e-10$	$5.9e-08$
1.0	$7.8250e-10$	$3.0e-08$

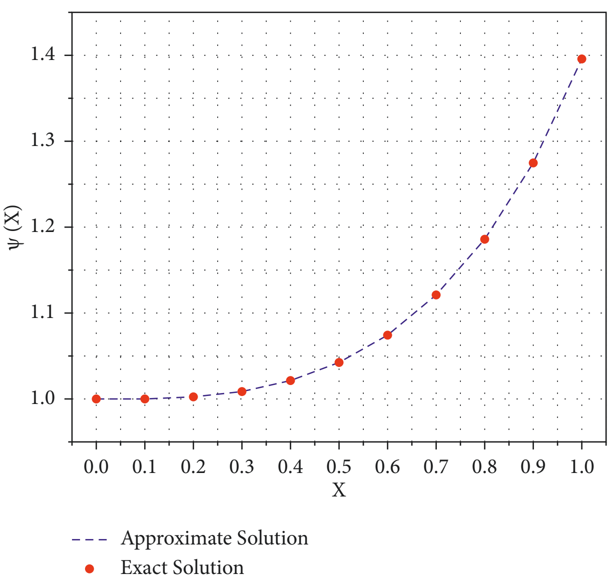

Figure 6: : Proposed and exact solutions for Problem 6.

Problem 6. [64] Finally, a special form based on the category 2 is considered for the third-order PD-LE model to compare the effectiveness of the proposed algorithm in the form as

$$\begin{cases} \dfrac{d^3}{dx^3}\Psi(x) + \dfrac{4}{x}\dfrac{d^2}{dx^2}\Psi(x) - \left(x^6 + 10x^3 + 10\right)\psi(x) = 0, \\ \Psi(0) = 1, \\ \dfrac{d\Psi(0)}{dx} = \dfrac{d^2\Psi(0)}{dx^2} = 0. \end{cases} \quad (52)$$

The exact solution of (52) is $\Psi(x) = e^{x^3/3}$. We test our proposed algorithm for acquiring the results and compare these results to the results in [52] in Table 10. As can be seen, from these results, our method gives a better solution compared to the other methods. Also, Figure 6 illustrates the behavior of the solution compared to the exact one, and they are in perfect agreement with each other. In addition, the consumed time for the data is found to be 3.511 sec, but there is no reported CPU time in [52] to compare.

6. Conclusion

In this work, the design of a novel third kind of nonlinear pantograph differential Lane–Emden model is carried out using the pantograph differential model and the typical form of the Lane–Emden system. Two different categories of the novel model together with the shape factors, singular point values, and pantographs of each category are discussed in detail. The singularity at the origin performs twice in category 1, while a single singularity is observed in category 2. Likewise, the single shape factor exists in the typical Lane–Emden system, whereas the shape factor appeared twice in category 1, and the single shape factor is calculated in category 2. For the excellence of the novel system, numerical experimentations have been accomplished by applying the famous Bernoulli collocation approach. A detailed residual error analysis is performed to support the efficiency of the scheme. The operative outcomes have been achieved to solve the novel designed model applying the Bernoulli collocation approach. The absolute error plots and tables have been presented based on the obtained numerical values for $N = 6, 8, 10$. The satisfactory absolute error values for all four problems have been obtained, and one can observe that these values lie in 10^{-10} and 10^{-15}. One can determine based on these accessible observations that the designed singular model is accurate, and the numerical results are precise.

In the future, the Bernoulli collection scheme can be implemented to solve different nonlinear and higher-order models with real applications in different areas of science and engineering [65–69].

Data Availability

All data generated or analyzed during this study are included in this article.

Conflicts of Interest

The authors declare that they have no conflicts of interest.

Authors' Contributions

Waleed Adel conceptualized the study, developed the methodology, provided the software, performed data curation, and wrote the original draft. Zulqurnain Sabir wrote the original draft, performed data curation, and reviewed and edited the article. Hadi Rezazadeh performed supervision and reviewed and edited the article. A. Aldurayhim reviewed and edited the article and provided funding.

References

[1] D. S. Li and M. Z. Liu, "Exact solution properties of a multi-pantograph delay differential equation," *Journal of Harbin Institute of Technology*, vol. 32, no. 3, pp. 1–3, 2000.

[2] J. M. Cushing and K. Yang, "Delay differential equations with applications in population dynamics," *Bulletin of Mathematical Biology*, vol. 57, no. 1, p. 169, 1995.

[3] T. Zhao, “Global periodic-solutions for a differential delay system modeling a microbial population in the chemostat,” *Journal of Mathematical Analysis and Applications*, vol. 193, no. 1, pp. 329–352, 1995.

[4] W. Li, B. Chen, C. Meng et al., “Ultrafast all-optical graphene modulator,” *Nano Letters*, vol. 14, no. 2, pp. 955–959, 2014.

[5] S.-I. Niculescu, *Delay Effects on Stability: A Robust Control Approach*, Vol. 269, Springer Science & Business Media, , London, 2001.

[6] S. K. Vanani, J. S. Hafshejani, F. Soleymani, and M. Khan, On the Numerical Solution of Generalized Pantograph Equation,” *World Applied Sciences Journal*, vol. 13, 2011.

[7] L. Bogachev, G. Derfel, S. Molchanov, and J. Ochendon, “On bounded solutions of the balanced generalized pantograph equation,” in *Topics in Stochastic Analysis and Nonparametric Estimation*, vol. 145, pp. 29–49, Springer, New York, NY, 2008.

[8] Ş. Yüzbaşı and M. Karaçayır, “A Galerkin-like approach to solve multi-pantograph type delay differential equations,” *Filomat*, vol. 32, no. 2, pp. 409–422, 2018.

[9] S. Yüzbaşi and M. Karaçayir, “A galerkin-type method for solutions of pantograph-type Volterra Fredholm integro-differential equations with functional upper limit,” *Sigma Journal of Engineering and Natural Sciences*, vol. 38, no. 2, pp. 995–1005, 2020.

[10] M. Z. Liu and D. Li, “Properties of analytic solution and numerical solution of multi-pantograph equation,” *Applied Mathematics and Computation*, vol. 155, no. 3, pp. 853–871, 2004.

[11] M. A. Koroma, C. Zhan, A. F. Kamara, and A. B. Sesay, “Laplace decomposition approximation solution for a system of multi-pantograph equations,” *International Journal of Mathematical, Computational Science and Engineering*, vol. 7, no. 7, pp. 39–44, 2013.

[12] Ş. Yüzbaşi and N. Ismailov, “A Taylor operation method for solutions of generalized pantograph type delay differential equations,” *Turkish Journal of Mathematics*, vol. 42, no. 2, pp. 395–406, 2018.

[13] Ş. Yüzbaşı, “An efficient algorithm for solving multi-pantograph equation systems,” *Computers & Mathematics with Applications*, vol. 64, no. 4, pp. 589–603, 2012.

[14] Ş. Yüzbaşı and M. Sezer, “An exponential approximation for solutions of generalized pantograph-delay differential equations,” *Applied Mathematical Modelling*, vol. 37, no. 22, pp. 9160–9173, 2013.

[15] Ş. Yüzbaşı and M. Sezer, “Shifted Legendre approximation with the residual correction to solve pantograph-delay type differential equations,” *Applied Mathematical Modelling*, vol. 39, no. 21, pp. 6529–6542, 2015.

[16] I. Khan, M. A. Z. Raja, M. A. R. Khan, M. Shoaib, S. Islam, and Z. Shah, “Design of backpropagated intelligent networks for nonlinear second-order lane-emden pantograph delay differential systems,” *Arabian Journal for Science and Engineering*, vol. 47, no. 2, pp. 1197–1210, 2022.

[17] Z. Sabir, H. A. Wahab, H. A. Wahab, and J. L. G. Guirao, “A novel design of Gudermannian function as a neural network for the singular nonlinear delayed, prediction and pantograph differential models,” *Mathematical Biosciences and Engineering*, vol. 19, no. 1, pp. 663–687, 2021.

[18] Ş. Yüzbaşı, G. Emrah, and M. Sezer, “Residual correction of the Hermite polynomial solutions of the generalized pantograph equations,” *New Trends in Mathematical Sciences*, vol. 3, no. 2, pp. 118–125, 2015.

[19] M. Izadi, Ş. Yüzbaşı, and K. J. Ansari, “Application of vieta-lucas series to solve a class of multi-pantograph delay differential equations with singularity,” *Symmetry*, vol. 13, no. 12, p. 2370, 2021.

[20] Z. Sabir, M. A. Z. Raja, D. N. Le, and A. A. Aly, “A neuro-swarming intelligent heuristic for second-order nonlinear Lane-Emden multi-pantograph delay differential system,” *Complex & Intelligent Systems*, vol. 8, pp. 1–14, 2021.

[21] Z. Sabir, D. Baleanu, M. A. Z. Raja, and J. L. G. Guirao, “Design of neuro-swarming heuristic solver for multi-pantograph singular delay differential equation,” *Fractals*, vol. 29, no. 5, Article ID 2140022, 2021.

[22] K. Nisar, Z. Sabir, M. A. Z. Raja et al., “Design of Morlet Wavelet Neural Network for Solving a Class of Singular Pantograph Nonlinear Differential Models,” *IEEE Access*, vol. 9, 2021.

[23] C. Phang, Y. T. Toh, and F. S. Md Nasrudin, “An operational matrix method based on poly-Bernoulli polynomials for solving fractional delay differential equations,” *Computation*, vol. 8, no. 3, p. 82, 2020.

[24] D. Flockerzi and K. Sundmacher, “On coupled Lane-Emden equations arising in dusty fluid models,” *Journal of Physics: Conference Series*, vol. 268, no. 1, Article ID 012006, 2011.

[25] V. B. Mandelzweig and F. Tabakin, “Quasilinearization approach to nonlinear problems in physics with application to nonlinear ODEs,” *Computer Physics Communications*, vol. 141, no. 2, pp. 268–281, 2001.

[26] R. Rach, J.-S. Duan, and A.-M. Wazwaz, “Solving coupled Lane-Emden boundary value problems in catalytic diffusion reactions by the Adomian decomposition method,” *Journal of Mathematical Chemistry*, vol. 52, no. 1, pp. 255–267, 2014.

[27] T. Luo and Z. Xin, H. Zeng, Nonlinear asymptotic stability of the lane-emden solutions for the viscous gaseous star problem with degenerate density dependent viscosities,” *Communications in Mathematical Physics*, vol. 347, no. 3, pp. 657–702, 2016.

[28] K. Boubaker and R. A. Van Gorder, “Application of the BPES to Lane-Emden equations governing polytropic and isothermal gas spheres,” *New Astronomy*, vol. 17, no. 6, pp. 565–569, 2012.

[29] J. A. Khan, M. A. Z. Raja, M. M. Rashidi, M. I. Syam, A. M. Wazwaz, and A. M. Wazwaz, “Nature-inspired computing approach for solving non-linear singular Emden-Fowler problem arising in electromagnetic theory,” *Connection Science*, vol. 27, no. 4, pp. 377–396, 2015.

[30] J. I. Ramos, “Linearization methods in classical and quantum mechanics,” *Computer Physics Communications*, vol. 153, no. 2, pp. 199–208, 2003.

[31] A. H. Bhrawy, A. S. Alofi, and R. A. Van Gorder, “An efficient collocation method for a class of boundary value problems arising in mathematical physics and geometry,” *Abstract and Applied Analysis*, vol. 2014, Article ID 425648, 9 pages, 2014.

[32] M. Dehghan and F. Shakeri, “Solution of an integro-differential equation arising in oscillating magnetic fields using He’s homotopy perturbation method,” *Progress in Electromagnetics Research*, vol. 78, pp. 361–376, 2008.

[33] A. Taghavi and S. Pearce, “A solution to the Lane-Emden equation in the theory of stellar structure utilizing the Tau method,” *Mathematical Methods in the Applied Sciences*, vol. 36, no. 10, pp. 1240–1247, 2013.

[34] V. Rădulescu and D. Repovš, “Combined effects in nonlinear problems arising in the study of anisotropic continuous media,” *Nonlinear Analysis: Theory, Methods & Applications*, vol. 75, no. 3, pp. 1524–1530, 2012.

[35] A.-M. Wazwaz, "A new algorithm for solving differential equations of Lane–Emden type," *Applied Mathematics and Computation*, vol. 118, no. 2-3, pp. 287–310, 2001.
[36] Z. Sabir, M. A. Z. Raja, C. M. Khalique, and C. Unlu, "Neuro-evolution computing for nonlinear multi-singular system of third order Emden-Fowler equation," *Mathematics and Computers in Simulation*, vol. 185, pp. 799–812, 2021.
[37] K. Nisar, M. A. Z. Sabir, A. A. A Ibrahim et al., "Evolutionary integrated heuristic with gudermannian neural networks for second kind of lane-emden nonlinear singular models," *Applied Sciences*, vol. 11, no. 11, p. 4725, 2021.
[38] Z. Sabir, H. A. Wahab, M. Umar, M. G. Sakar, and M. A. Z. Raja, "Novel design of Morlet wavelet neural network for solving second order Lane-Emden equation," *Mathematics and Computers in Simulation*, vol. 172, pp. 1–14, 2020.
[39] P. Roul, "A fourth-order non-uniform mesh optimal B-spline collocation method for solving a strongly nonlinear singular boundary value problem describing electrohydrodynamic flow of a fluid," *Applied Numerical Mathematics*, vol. 153, pp. 558–574, 2020.
[40] Z. Sabir, M. R. Ali, R. S. Muhammad Asif Zahoor Raja, and B. Dumitru, *Dynamics of Three-point Boundary Value Problems with Gudermannian Neural Networks*, pp. 1–13, Evolutionary Intelligence, Germany, 2022.
[41] P. Roul, "A new mixed MADM-Collocation approach for solving a class of Lane-Emden singular boundary value problems," *Journal of Mathematical Chemistry*, vol. 57, no. 3, pp. 945–969, 2019.
[42] Z. Sabir, D. Baleanu, M. R. Ali, and R. Sadat, "A novel computing stochastic algorithm to solve the nonlinear singular periodic boundary value problems," *International Journal of Computer Mathematics*, pp. 1–14, 2022.
[43] P. Roul and K. Thula, "A fourth-order B-spline collocation method and its error analysis for Bratu-type and Lane-Emden problems," *International Journal of Computer Mathematics*, vol. 96, no. 1, pp. 85–104, 2019.
[44] H. Madduri and P. Roul, "A fast-converging iterative scheme for solving a system of Lane-Emden equations arising in catalytic diffusion reactions," *Journal of Mathematical Chemistry*, vol. 57, no. 2, pp. 570–582, 2019.
[45] Z. Sabir, M. A. Z. Raja, T. G. Nguyen, I. Fathurrochman, R. Sadat, and M. R. Ali, "Applications of neural networks for the novel designed of nonlinear fractional seventh order singular system," *The European Physical Journal - Special Topics*, pp. 1–15, 2022.
[46] P. Roul, H. Madduri, and R. Agarwal, "A fast-converging recursive approach for Lane-Emden type initial value problems arising in astrophysics," *Journal of Computational and Applied Mathematics*, vol. 359, pp. 182–195, 2019.
[47] P. Roul and V. M. K. Prasad Goura, "B-spline collocation methods and their convergence for a class of nonlinear derivative dependent singular boundary value problems," *Applied Mathematics and Computation*, vol. 341, pp. 428–450, 2019.
[48] Z. Sabir, M. A. Z. Raja, M. Shoaib, R. Sadat, and M. R. Ali, "A novel design of a sixth-order nonlinear modeling for solving engineering phenomena based on neuro intelligence algorithm," *Engineering with Computers*, pp. 1–16, 2022.
[49] P. Roul, K. Thula, and R. Agarwal, "Non-optimal fourth-order and optimal sixth-order B-spline collocation methods for Lane-Emden boundary value problems," *Applied Numerical Mathematics*, vol. 145, pp. 342–360, 2019.
[50] W. Adel and Z. Sabir, "Solving a new design of nonlinear second-order Lane-Emden pantograph delay differential model via Bernoulli collocation method," *The European Physical Journal Plus*, vol. 135, no. 5, p. 427, 2020.
[51] E. Tohidi and A. Kılıçman, "A collocation method based on the Bernoulli operational matrix for solving nonlinear BVPs which arise from the problems in calculus of variation," *Mathematical Problems in Engineering*, 2013.
[52] M. Erfanian and H. Zeidabadi, "Solving two-dimensional nonlinear mixed Volterra Fredholm integral equations by using rationalized Haar functions in the complex plane," *Journal of Mathematical Modeling*, vol. 7, no. 4, 2019.
[53] Q. Ren and H. Tian, "Numerical solution of the static beam problem by Bernoulli collocation method," *Applied Mathematical Modelling*, vol. 40, pp. 8886–8897, 2016.
[54] F. Toutounian, E. Tohidi, and S. Stanford, "A collocation method based on the Bernoulli operational matrix for solving high-order linear complex differential equations in a rectangular domain," *Abstract and Applied Analysis*, vol. 2013, Article ID 823098, 12 pages, 2013.
[55] N. Moshtaghi and A. Saadatmandi, "Numerical solution of time fractional cable equation via the sinc-Bernoulli collocation method," *Journal of Applied and Computational Mechanics*, vol. 7, no. 4, pp. 1916–1924, 2021.
[56] M. El-Gamel, W. Adel, and M. S. El-Azab, "Eigenvalues and eigenfunctions of fourth-order sturm-liouville problems using Bernoulli series with Chebychev collocation points," *Mathematical Sciences*, vol. 8, pp. 1–8, 2021.
[57] N. Samadyar and F. Mirzaee, "Orthonormal Bernoulli polynomials collocation approach for solving stochastic Itô-Volterra integral equations of Abel type," *International Journal of Numerical Modelling: Electronic Networks, Devices and Fields*, vol. 33, Article ID e2688, 2020.
[58] S. Bazm and A. Hosseini, "Bernoulli operational matrix method for the numerical solution of nonlinear two-dimensional Volterra–Fredholm integral equations of Hammerstein type," *Computational and Applied Mathematics*, vol. 39, no. 2, pp. 1–20, 2020.
[59] J. R. Loh and P. Chang, "Numerical solution of Fredholm fractional integro-differential equation with right-sided Caputo's derivative using Bernoulli polynomials operational matrix of fractional derivative," *Mediterranean Journal of Mathematics*, vol. 16, no. 2, pp. 1–25, 2019.
[60] K. Eriksson and V. Thomée, "Galerkin methods for singular boundary value problems in one space dimension," *Mathematics of Computation*, vol. 42, no. 166, pp. 345–367, 1984.
[61] M. El-Gamel and M. Sameeh, "Numerical solution of singular two-point boundary value problems by the collocation method with the Chebyshev bases," *SeMA Journal*, vol. 74, no. 4, pp. 627–641, 2017.
[62] M. Abramowitz and I. A. Stegun, *Handbook of Mathematical Functions with Formulas, Graphs, and Mathematical Tables*, John Wiley & Sons, New York, 1972.
[63] Z. Sabir, M. A. Z. Raja, M. Umar, and M. Shoaib, "Design of neuro-swarming-based heuristics to solve the third-order nonlinear multi-singular Emden–Fowler equation," *The European Physical Journal Plus*, vol. 135, no. 5, p. 410, 2020.
[64] Z. Sabir, M. Umar, J. L. G. Guirao, M. Shoaib, M. A. Z. Raja, and M.A. Z. Raja, "Integrated intelligent computing paradigm for nonlinear multi-singular third-order Emden-Fowler equation," *Neural Computing & Applications*, vol. 33, no. 8, pp. 3417–3436, 2021.
[65] Z. Sabir, S. Saoud, M. A. Z. Raja, H. A. Wahab, and A. Arbi, "Heuristic computing technique for numerical solutions of nonlinear fourth order Emden-Fowler equation,"

Mathematics and Computers in Simulation, vol. 178, pp. 534–548, 2020.

[66] A. Arbi, Y. Guo, and J. Cao, "Convergence analysis on time scales for HOBAM neural networks in the Stepanov-like weighted pseudo almost automorphic space," *Neural Computing & Applications*, vol. 33, no. 8, pp. 3567–3581, 2021.

[67] A. Arbi, "Novel traveling waves solutions for nonlinear delayed dynamical neural networks with leakage term," *Chaos, Solitons & Fractals*, vol. 152, Article ID 111436, 2021.

[68] Y. Guo, S. S. Ge, and A. Arbi, "Stability of traveling waves solutions for nonlinear cellular neural networks with distributed delays," *Journal of Systems Science and Complexity*, vol. 35, pp. 1–14, 2021.

[69] Z. Sabir, M. A. Z. Raja, A. Arbi, G. C. Altamirano, and J. Cao, "Neuro-swarms intelligent computing using Gudermannian kernel for solving a class of second order Lane-Emden singular nonlinear model," *AIMS Math*, vol. 6, no. 3, pp. 2468–2485, 2021.